R. J. Wilfinger

P. H. Bardell

D. S. Chhabra*

The Resonistor: A Frequency Selective Device Utilizing the Mechanical Resonance of a Silicon Substrate[†]

Abstract: This communication describes an approach to tuned monolithic circuitry which utilizes the mechanical resonance of a silicon substrate. The proposed device is compatible with monolithic technology and will operate from a few hundred cycles to hundreds of kilocycles. The basic device consists of a silicon cantilever mechanically deflected by electrically induced thermal expansion. Diffused silicon piezo-resistive elements are used to detect stress in the cantilever and provide an electrical output. Maximum stress and electrical output occur when the cantilever is driven at its mechanical resonant frequency.

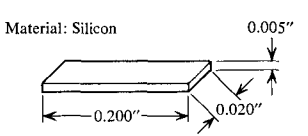
Quartz crystals, tuning forks and other resonant mechanical structures have long been used to control electronic circuits. Monolithic technology has created a renewed interest in mechanical structures because of the potential packaging densities achievable and inherent frequency stability.¹

This communication describes an approach to tuned monolithic circuitry which utilizes the mechanical resonance of a silicon substrate. The proposed device is compatible with monolithic technology and will operate from a few hundred cycles to hundreds of kilocycles. This basic device consists of a silicon cantilever mechanically deflected by electrically induced thermal expansion. Diffused silicon piezoresistive elements are used to detect stress in the cantilever and provide an electrical output. Maximum stress and electrical output occur when the cantilever is driven at its mechanical resonant frequency.

Mechanical configuration

The resonant frequency of mechanical structures is determined by the physical configuration and dimensions of the structure and the mechanical characteristics of the material. Figure 1 compares the resonant frequency of a number of common mechanical structures that may be used for the resonistor. The simple cantilever was chosen from size considerations and for ease of fabrication. Addition of a mass at the unsupported end provides a system with the lowest resonant frequency for given dimensions. The resonant frequency for the simple cantilever is given by:²

$$\omega_n = \sqrt{\frac{EBH^3}{4L^3(m+0.23m_c)}},$$
 (1)



		Natural resonant frequency in kHz		
Mode		Fundamental	1st overtone	2nd overtone
	Flexure: fixed-free	7.36	49.9	129.2
	Flexure: fixed—fixed	46.9	129.2	253.4
	Torsional	270	-	_
	Longitudinal	455		_

Figure 1 A comparison of the resonant frequencies obtained by exciting a $200 \times 20 \times 5$ mil silicon cantilever in various modes. The simple cantilever (fixed-free flexure) provides the lowest resonant frequency for given dimensions.

where

E =Young's modulus,

B = cantilever width,

H = cantilever thickness,

L = cantilever length,

 $m_c = \text{cantilever mass, and}$

m = end mass.

^{*} Present address: Stanford University, Stanford, Calif.

[†] Part of this paper was presented at the 1966 International Electron Devices Meeting at Washington, D. C., October 26-28, 1966.

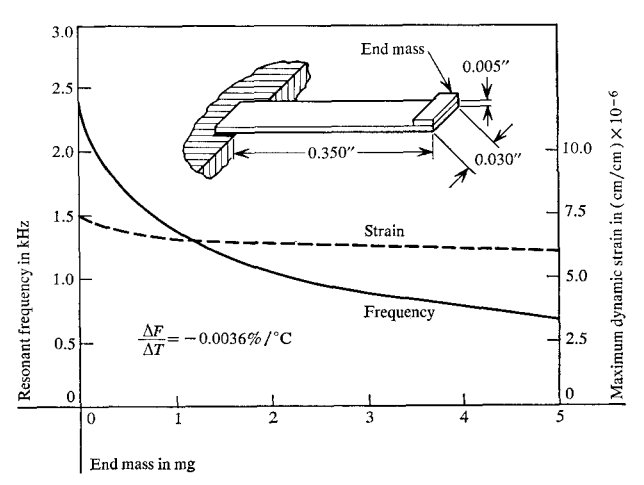


Figure 2 Resonant frequency and maximum dynamic strain (at supported end for 2.5 micron deflection at the unsupported end) calculated for a $350 \times 30 \times 5$ mil silicon cantilever. Temperature dependence is calculated to be 36 PPM/°C from changes in the elastic constants.

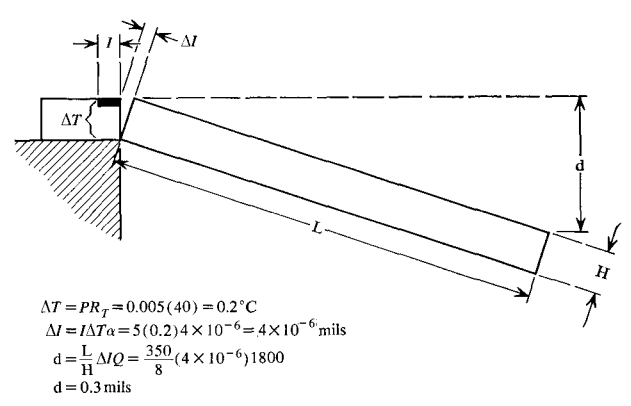


Figure 3 Simplified model of cantilever deflected by localized thermal expansion. The heated element has the dimension L. P, R_T and α represent the power dissipated in watts, the thermal resistance, and thermal coefficient of expansion, respectively.

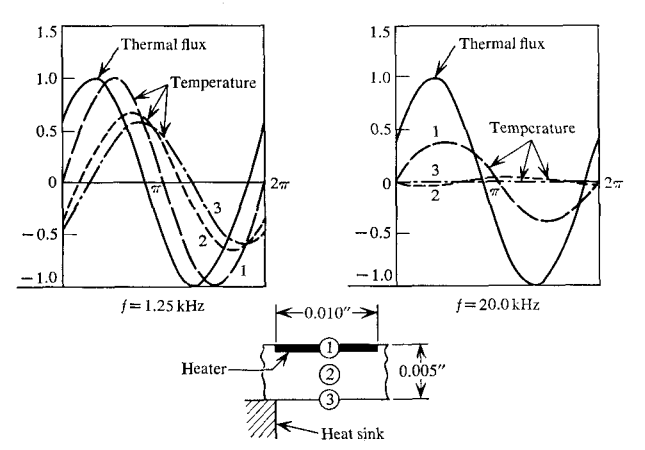


Figure 4 Temperature distribution calculated from two-dimensional heat flow model. Although the absolute temperature drops at higher frequencies, the temperature gradient across the thickness of the beam remains essentially constant up to 20 kHz for the configuration shown.

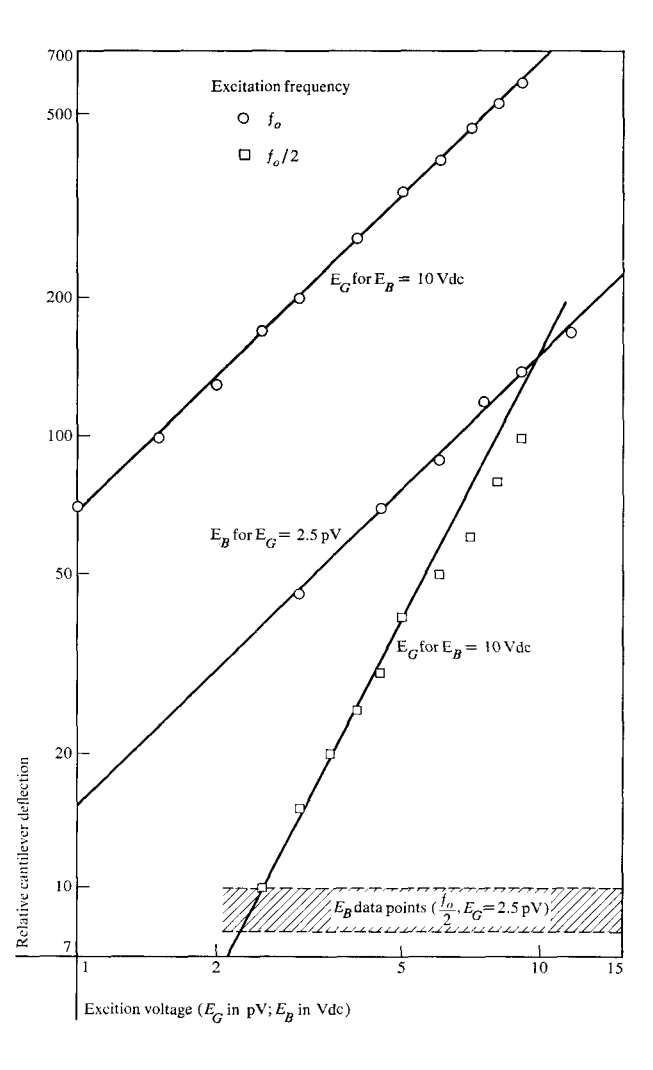


Figure 5 Experimentally observed cantilever deflection vs. input voltage at the resonant frequency and one-half the resonant frequency. The slopes and ratio of deflections for the two frequencies are in good agreement with Eq. (2). Deflection is directly proportional to E_G .

Figure 2 shows the resonant frequency and maximum dynamic strain, as a function of end mass, calculated for the silicon cantilever in the inset. The temperature coefficient of frequency is dominated by the change in the elastic constants and is calculated to be 36 ppm/°C.

Mechanical excitation

Silicon does not exhibit the piezoelectric effect and its electrostriction coefficient is too small to be of practical benefit. Electrically induced thermal expansion was investigated and found to be quite effective as an electrical-to-mechanical conversion mechanism.

A temperature gradient within a silicon cantilever will cause localized thermal expansion and a deflection moment.

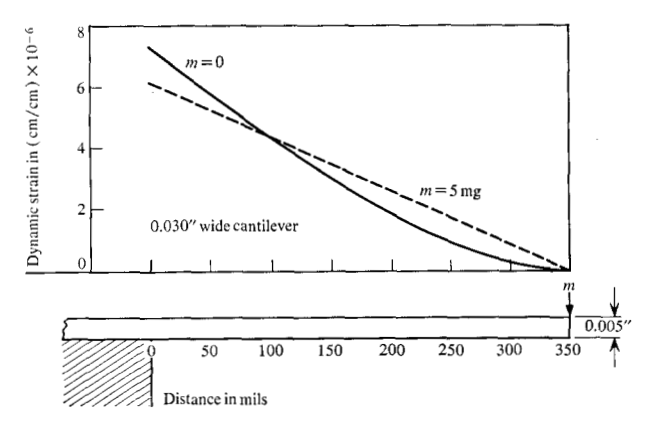


Figure 6 Calculated value of dynamic strain along length of cantilever. Distribution approaches linearity as end mass approaches mass of cantilever.

The desired gradient has been produced by electrical power dissipation in a diffused resistor located near the cantilever support. Figure 3 shows a simplified model of a cantilever being deflected by a localized thermal element. From this model, a deflection of 40 Å is calculated at 5 mW for the dimensions shown. The deflection when driven to resonance becomes Q times this value or 7.5μ for a cantilever with a Q of 1800.

The temperature distribution within the bulk of the cantilever was analyzed in two dimensions. Figure 4 shows the temperature obtained at three key points from the heat flow calculation. These results indicate that a practical temperature gradient may be maintained at 20 kHz for the structure shown

Dissipating ac power in a diffused resistor will cause the surface temperature near that resistor to change at a periodic rate. This change is localized within a thin skin at the surface.³ The depth of the skin, in silicon, is about 6 mils at 1 kHz and is inversely proportional to the square root of frequency. The ac component of the power dissipated in the excitation resistor is given by:

$$P_{AC} = \frac{2E_B E_G}{R} \sin \omega t - \frac{E_G^2}{2R} \cos 2\omega t , \qquad (2)$$

where E_B is the dc voltage and E_G the peak value of the superimposed sinusoidal voltage. When the excitation frequency coincides with the natural resonant frequency of the cantilever, deflections of the order of microns have been observed.

Figure 5 shows the excellent agreement obtained between the power calculated in Eq. (2) and the experimentally measured cantilever deflection. Equation (2) and the experimental results of Fig. 5 show that the deflection is directly proportional to the excitation voltage.

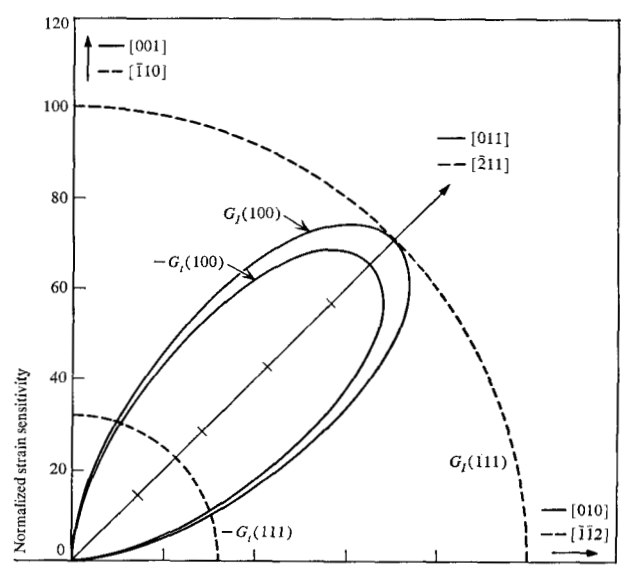
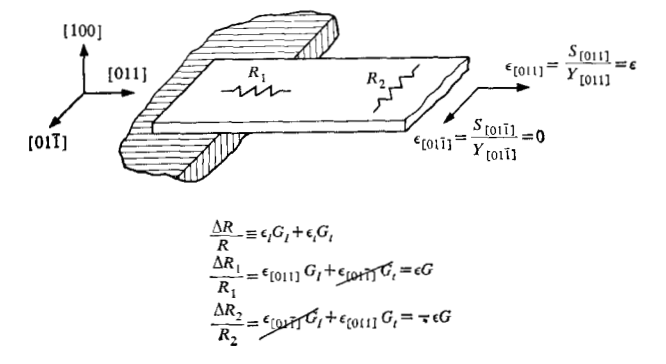


Figure 7 Stress sensitivity as a function of crystallographic orientation in (100) face (solid lines) and (111) face (dashed lines). The (100) face makes possible fabrication of piezoresistive elements having approximately equal but opposite signs.

Figure 8 Relative position of piezoresistive elements with respect to the crystallographic axis in the (100) face. The signs for the longitudinal and transverse sensitivity factors were taken from Fig. 7.



Sensing resonance

Resonance is accompanied by maximum deflection and stress and this stress is concentrated near the supported end (see Fig. 6). Piezoresistive elements provide a sensitive indication of stress and are conveniently fabricated in silicon by diffusion. Figure 7 compares the stress sensitivity of piezoresistive elements oriented in the (100) and (111) crystallographic faces. From Figs. 7 and 8, it can be seen that by properly orienting the piezoresistive elements with respect to the crystallographic directions in the (100) face, elements with maximum stress sensitivity but opposite signs may be

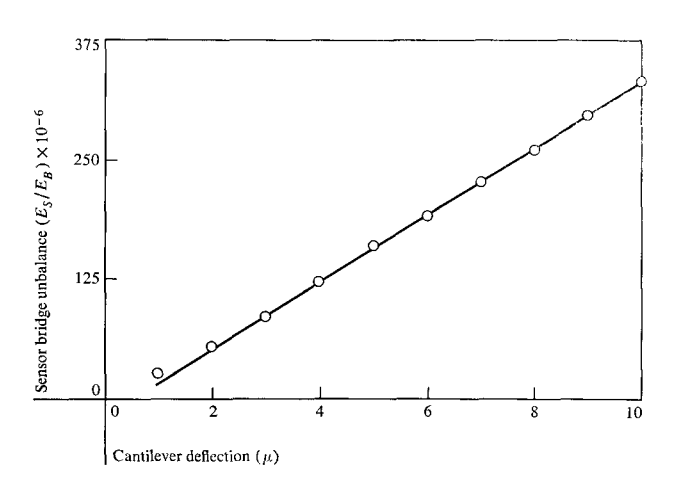


Figure 9 Measured sensor bridge imbalance as a function of cantilever deflection. Linear output in conjunction with linear excitation characteristics shown in Fig. 5 provide desired total linear electrical characteristics.

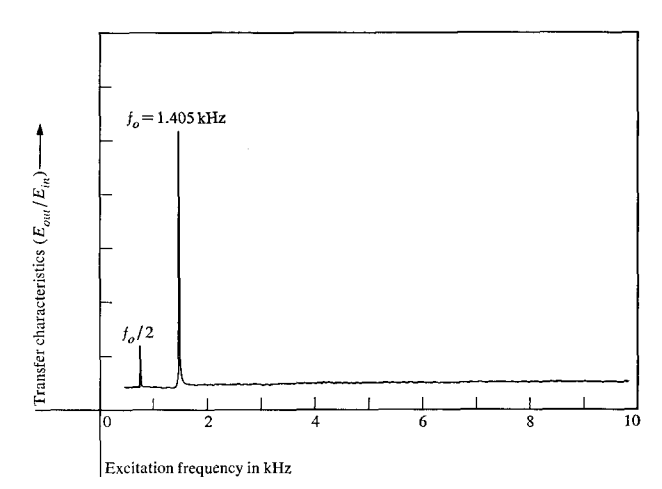


Figure 12 Experimentally measured voltage transfer characteristics as a function of excitation frequency for a typical device. The origin of the peak measured at one-half the resonant frequency is evident from examination of (2).

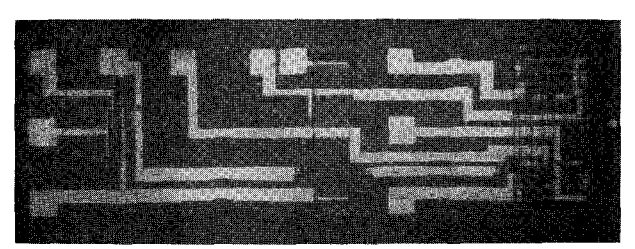
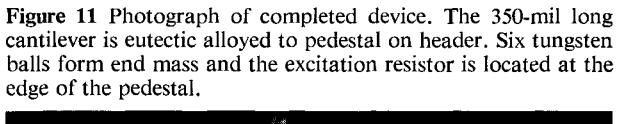
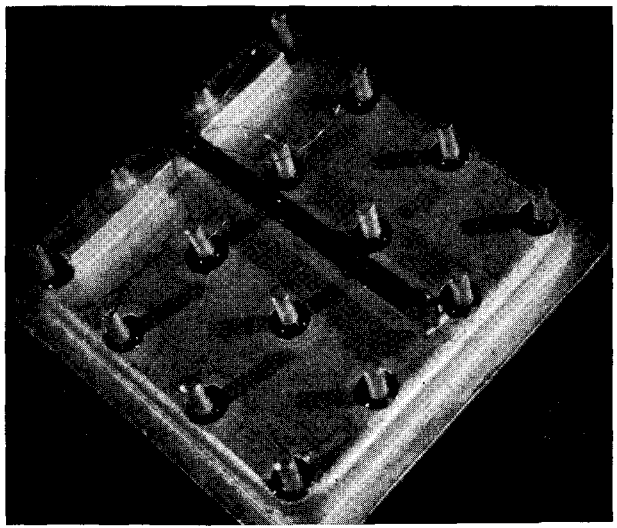


Figure 10 Photograph of monolithic circuit pattern. Circuit consists of transistor driver, excitation resistor in collector lead, and four piezoresistive elements wired in bridge pattern. Pattern is 96×32 mils.





fabricated. Two elements of each sign may be wired to form a bridge circuit which has maximum stress sensitivity and rejects the common mode stray electrical coupling and temperature change. Figure 9 shows the output measured from such a bridge as a function of cantilever deflection. The experimental results shown in Figs. 5 and 9 indicate that the electrical output of the resonistor is directly proportional to the electrical input. This is a highly desirable characteristic if the device is to be used in linear circuit applications.

Device fabrication and characteristics

The pattern shown in Fig. 10 was processed in the n type epitaxial layer of a p type silicon substrate using standard monolithic techniques. The pattern consists of four piezoresistors and a transistor in the common-emitter configuration with a 360 Ω excitation resistor in the collector. All resistors were formed during the base diffusion. Cantilevers 350 X 30 mils were cut from the 8 mil thick wafer and eutecticalloyed to a gold plated pedestal. Figure 11 shows a mounted device. The pattern is placed so that the transistor is on the pedestal with the excitation resistor located at the edge of the pedestal. The 3.6 k Ω piezoresistive elements are located further out on the cantilever. Devices mounted in this way have a resonant frequency of 3.2 kHz and a Q of 1400. Adding a 3 mg mass to the unsupported end of the cantilever decreases frequency to 1.4 kHz and increases the Q to about 2500. The voltage transfer ratio of this device is 0.2 to 0.3 for a collector dc supply current of 6 mA and with a bridge supply voltage of 6 V dc.

Figure 12 shows the voltage transfer ratio of a typical resonistor as a function of excitation frequency. The ratio

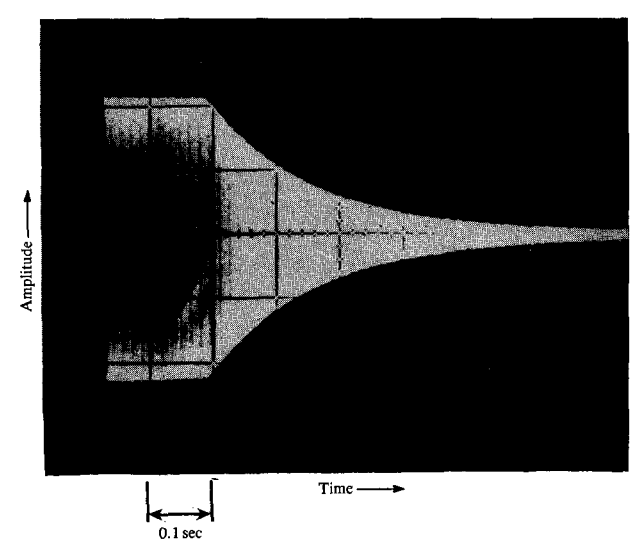
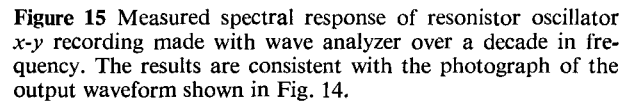
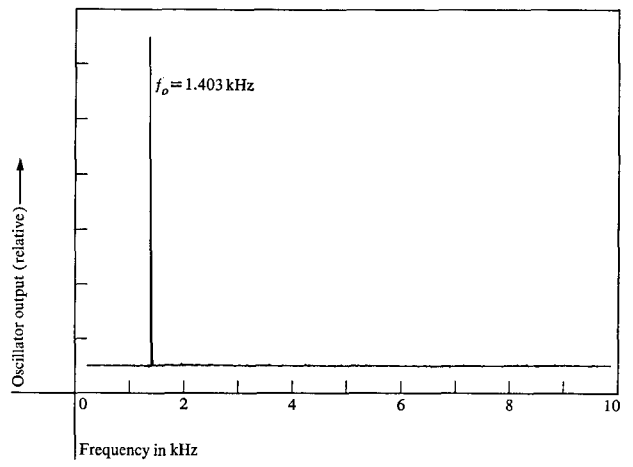


Figure 13 Display of free decay characteristics of a device. Device Q is 1800, which corresponds to a bandwidth of 1.8 Hz at the resonant frequency of 3.2 kHz.





of output signal at resonance to the output signal at excitation frequencies outside the pass envelope is typically 25 to 1 and greater. Figure 13 shows the free decay characteristics of a device with a Q of 1800.

By coupling the output to the input of a resonistor with an amplifier of sufficient gain to overcome the insertion loss of the device at resonance, sustained oscillation was obtained. Figure 14 shows the input and output waveforms observed at the terminals of the device in oscillation. The driving waveform has been purposely distorted to better illustrate the properties of the device. The spectrum analysis shown in Fig. 15 indicates the degree of purity obtained with

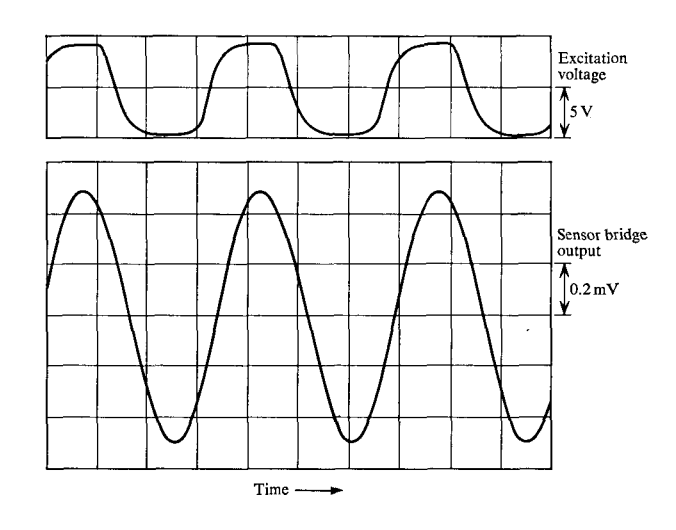
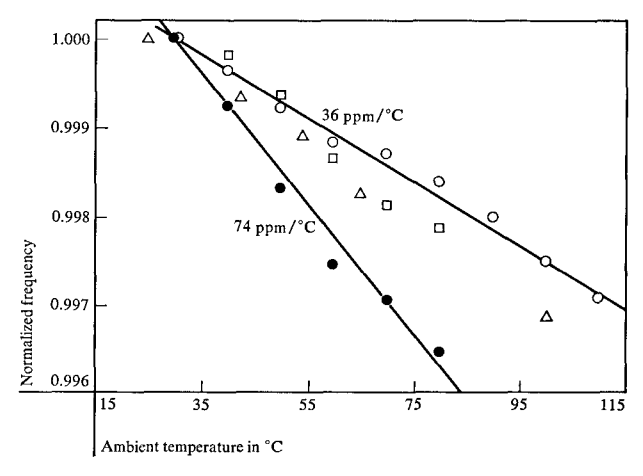


Figure 14 Experimentally observed input and output voltage wave-forms for the device in oscillation, Frequency of oscillation is 1.403 kHz.

Figure 16 Measured frequency drift with temperature of representative devices. Results compare favorably with the predicted value of 36 ppm/°C.



the device. The measured frequency drift with temperature of four representative resonistor-controlled oscillators is shown in Fig. 16. The results compare favorably with the predicted value of 36 ppm/°C, calculated using the temperature coefficients of the elastic constants of silicon.⁵

Summary

Resonistors have been fabricated in the range from 600 Hz to 200 kHz. The devices were fabricated from similar wafers and differed only in mechanical dimensions and end loading. The 200 kHz device exhibited a Q of 250 and a voltage transfer ratio of 0.01. The cantilever is $50 \times 30 \times 8$ mils

and unloaded. In the one to two kHz range devices with Q's as high as 4400 have been observed.

Completely integrated low frequency oscillators are attainable with this technique. The resulting oscillators will have stable characteristics, high packaging densities and benefit from the economies of monolithic technology.

Acknowledgments

The authors would like to gratefully acknowledge the contributions of L. A. Davidson and the experimental support of R. Carballo.

References

- W. E. Newell, "Ultrasonics in Integrated Electronics," Proc. IEEE 53, 1305 (1965).
- C. M. Harris and C. E. Crede, Shock and Vibration Handbook, McGraw-Hill Publishing Co. Inc., New York, 1961, pp. 1-13.
- H. S. Carslaw, and J. C. Jaeger, Conduction of Heat in Solids, Oxford University Press, London 1959, p. 64.
- O. N. Tufte and D. Long, "Recent Developments in Semiconductor Piezoresistive Devices," Solid-State Electronics 6, 323 (1963).
- H. J. McSkimin et al., "Measurement of the Elastic Constants of Silicon Single Crystals and Their Thermal Constants," *Phys. Rev.* 83, 1080 (1951).

Received July 10, 1967.